θ_{23} octant measurement in 3+1 neutrino oscillations in T2HKK

Naoyuki Haba, Yukihiro Mimura, and Toshifumi Yamada◉

Institute of Science and Engineering, Shimane University, Matsue 690-8504, Japan

It has been pointed out that the mixing of an eV-scale sterile neutrino with active flavors can lead to a loss of sensitivity to the θ_{23} octant (sign of $\sin^2\theta_{23} - 1/2$) in long baseline experiments, because the main oscillation probability $P_0 = 4\sin^2\theta_{23}\sin^2\theta_{13}\sin^2\Delta_{31}$ can be degenerate with the sum of the interferences with the solar oscillation amplitude and an active-sterile oscillation amplitude in both neutrino and antineutrino oscillations, depending on the CP phases. In this paper, we show that the above degeneracy is resolved by measuring the same beam at different baseline lengths. We demonstrate that the Tokai-to-Hyper-Kamiokande-to-Korea (T2HKK) experiment (one 187 kton fiducial volume water Cerenkov detector is placed at Kamioka, $L = 295$ km, and another detector is put in Korea, $L \sim 1000$ km) exhibits a better sensitivity to the θ_{23} octant in those parameter regions where the experiment with the two detectors at Kamioka is insensitive to it. Therefore, if a hint of sterile-active mixings is discovered in short baseline experiments, T2HKK is a better option than the plan of placing two detectors at Kamioka. We also consider an alternative case where one detector is placed at Kamioka and a different detector is at Oki Islands, $L = 653$ km, and show that this configuration also leads to a better sensitivity to the θ_{23} octant.

I. INTRODUCTION

The octant of the neutrino mixing angle θ_{23}, namely, the sign of $\sin^2\theta_{23} - 1/2$, has profound implications for the SO(10) grand unification theory with renormalizable Yukawa couplings (see, e.g., Refs. [1–3]). Since ν_e and ν_μ disappearance channels are almost solely sensitive to $\sin^2(2\theta_{23})$, the best way to determine the octant is to use the $\nu_\mu \to \nu_e$ channel in long baseline experiments. For the standard three-flavor oscillations, the octant measurement has been investigated in Refs. [4–15].

It has been pointed out that if an eV-scale light sterile neutrino mixes with active flavors, it can considerably deteriorate the sensitivity of long baseline experiments to the θ_{23} octant [16].[1] This is based on the following observation: In the standard three-flavor oscillations, the part of the $\nu_\mu \to \nu_e$ oscillation probability sensitive to the θ_{23} octant, $P_0 = 4\sin^2\theta_{23}\sin^2\theta_{13}\sin^2\Delta_{31}$ ($\Delta_{31} \equiv \Delta m_{31}^2 L/(4E)$), is possibly mimicked by the interference of the solar and atmospheric oscillation amplitudes, $P_1 \simeq 4\sin\theta_{13}\sin\theta_{12}\times \cos\theta_{12}(\Delta m_{21}^2/\Delta m_{31}^2)\Delta_{31}\sin\Delta_{31}\cos(\Delta_{31} \pm \phi_{13})$, in either neutrino oscillations or antineutrino oscillations depending

on the CP phase ϕ_{13}, but not in both oscillations. Hence, a combination of neutrino- and antineutrino-focusing operations resolves the above degeneracy. In the $3 + 1$ oscillations, however, the interference of atmospheric and active-sterile oscillation amplitudes generates a new term, $P_2 \simeq 4\sin\theta_{14}\sin\theta_{24}\sin\theta_{13}\sin\theta_{23}\sin\Delta_{31}\sin(\Delta_{31} \pm \phi_{13} \mp \phi_{14})$. The sum $P_1 + P_2$ can mimic P_0 in both neutrino and antineutrino oscillations for some values of ϕ_{13} and ϕ_{14}, leading to a loss of sensitivity to the θ_{23} octant.

In this paper, we pursue the possibility that a combination of neutrino- and antineutrino-focusing operations *and* measurements of the same beam at different baseline lengths resolves the degeneracy of P_0 and $P_1 + P_2$, thereby resurrecting the sensitivity to the θ_{23} octant in the $3 + 1$ oscillations. For concreteness, we concentrate on the Tokai-to-Hyper-Kamiokande-to-Korea (T2HKK) experiment [25] (for early proposals, see Refs. [5,26–33]), where one 187 kton fiducial volume water Cerenkov detector is placed at Kamioka ($L = 295$ km) and another 187 kton detector is in Korea ($L \sim 1000$ km), which is a proposed extension of the Tokai-to-Hyper-Kamiokande (T2HK) experiment [34]. We conduct a comparative study of the T2HKK experiment with the plan of placing two 187 kton detectors at Kamioka. We will demonstrate that for some values of CP phases ϕ_{13} and ϕ_{14}, the sensitivity to the θ_{23} octant is lost in the latter experiment while the sensitivity is maintained in T2HKK, in spite of smaller statistics of T2HKK (as the baseline to Korea is longer than that to Kamioka). We further consider an alternative plan of placing a modest detector at Oki Islands [35–38] ($L = 653$ km) in addition to one 187 kton

---

[1]Recent studies on the impact of sterile-active mixings on long baseline experiments are Refs. [17–24].

detector at Kamioka and study how the sensitivity to the θ_{23} octant changes in this case.

Previously, the sensitivity of T2HK and T2HKK to the θ_{23} octant in the presence of mixings of an eV-scale sterile neutrino has been studied in Ref. [21]. Our study differs from it in that we consider both cases with $\theta_{34} = 0$ and $\theta_{34} \neq 0$ and further separately investigate the dependence of the sensitivity on θ_{34} and that on θ_{24}.[2] In contrast, Ref. [21] only assumes substantially large values for θ_{34} and varies $\theta_{34}, \theta_{14},$ θ_{24} only simultaneously. As we show in the main text, nonzero values of θ_{34} tend to increase the sensitivity to the θ_{23} octant, and hence, it is important to scrutinize the case with $\theta_{34} = 0$, which is the "worst situation" for the θ_{23} octant measurement. Also, since the sensitivity tends to increase with θ_{34} and decrease with θ_{24}, the dependences on θ_{34} and θ_{24} must be analyzed separately.

This paper is organized as follows: In Sec. II, we write the $\nu_\mu \to \nu_e$ oscillation probability in the $3 + 1$ oscillations, spot the terms that can lead to loss of sensitivity to θ_{23}

octant, and qualitatively state that this problem is mitigated in the T2HKK experiment. In Sec. III, we confirm the above qualitative statement through a numerical analysis. Section IV summarizes the paper.

II. 3+1 OSCILLATION PROBABILITY

We postulate the presence of one isospin-singlet neutrino, ν_s, that mixes with the three active flavors $(\nu_e, \nu_\mu, \nu_\tau)$ and yields four mass eigenstates $(\nu_1, \nu_2, \nu_3, \nu_4)$. We also assume that the mass of ν_4 is around 1 eV, and thus, ν_4 participates in oscillations in a J-PARC beam.

We parametrize the mixing of $(\nu_e, \nu_\mu, \nu_\tau, \nu_s)$ as follows:

$$|\nu_\alpha\rangle = \sum_{k=1}^{4} (U)_{\alpha k} |\nu_k\rangle \qquad (\alpha = e, \mu, \tau, s), \qquad (1)$$

with U being a 4×4 unitary matrix defined as

$$U = U_{34} U_{24} U_{14} U_{23} U_{13} U_{12},$$
$$(U_{ab})_{ij} = \delta_{ia}\delta_{ja}\cos\theta_{ab} + \delta_{ib}\delta_{jb}\cos\theta_{ab} + \delta_{ia}\delta_{jb}e^{-i\phi_{ab}}\sin\theta_{ab} - \delta_{ib}\delta_{ja}e^{i\phi_{ab}}\sin\theta_{ab}.$$
$$(a, b = 1, 2, 3, 4; a < b).$$

$U_{23}U_{13}U_{12}$ corresponds to a Pontecorvo-Maki-Nakagawa-Sakata matrix [39,40]. Henceforth, we fix the phase convention such that $\phi_{12} = \phi_{23} = \phi_{24} = 0$. Also, we take $\theta_{14} \geq 0, \theta_{24} \geq 0, \theta_{34} \geq 0$.

The probability of $\nu_\mu \to \nu_e$ oscillation, which is crucial for the θ_{23} octant measurement, is given by

$$P(\nu_\mu \to \nu_e) = \left| \left[\exp\left(-i \int_0^L dx\, H(x) \right) \right]_{12} \right|^2,$$

$$H(x) = \frac{1}{2E} U \begin{pmatrix} 0 & 0 & 0 & 0 \\ 0 & \Delta m_{21}^2 & 0 & 0 \\ 0 & 0 & \Delta m_{31}^2 & 0 \\ 0 & 0 & 0 & \Delta m_{41}^2 \end{pmatrix} U^\dagger + \begin{pmatrix} V_{cc} + V_{nc} & 0 & 0 & 0 \\ 0 & V_{nc} & 0 & 0 \\ 0 & 0 & V_{nc} & 0 \\ 0 & 0 & 0 & 0 \end{pmatrix}, \qquad (2)$$

where L is the baseline length, E is the neutrino energy, and $\Delta m_{i1}^2 = m_i^2 - m_1^2$. V_{cc} and V_{nc} denote the potentials generated by charged and neutral current interactions, respectively, which are evaluated as $V_{cc} = -2V_{nc} \simeq 0.193 \times 10^{-3} (\rho/(\text{g/cm}^3))/\text{km}$ with ρ being the matter density. The antineutrino oscillation probability $P(\bar{\nu}_\mu \to \bar{\nu}_e)$ is obtained by flipping the signs of $\phi_{13},$ $\phi_{14}, \phi_{34}, V_{cc}, V_{nc}$.

To gain physical insight, we expand Eq. (2) in the leading order of $\Delta m_{21}^2 L/E$, θ_{14}, θ_{24}, θ_{34}, and the matter effect (approximated to be uniform), and further take an average over $\Delta m_{41}^2 L/(4E)$ oscillations. The $\nu_\mu \to \nu_e$ and $\bar{\nu}_\mu \to \bar{\nu}_e$ oscillation probabilities are then written as

$$P(\overset{(-)}{\nu}_\mu \to \overset{(-)}{\nu}_e) \simeq 4\sin^2\theta_{13}\sin^2\theta_{23}\sin^2\left(\frac{\Delta m_{31}^2 L}{4E} \right)$$

$$+ 4\sin\theta_{13}\sin\theta_{12}\cos\theta_{12}\sin(2\theta_{23})\frac{\Delta m_{21}^2 L}{4E}\sin\left(\frac{\Delta m_{31}^2 L}{4E} \right)\cos\left(\frac{\Delta m_{31}^2 L}{4E} \pm \phi_{13} \right)$$

---

[2]Since the impact of sterile-active mixings on the θ_{23} octant measurement appears only in the combinations $\sin\theta_{14}\sin\theta_{24}$ and $\sin\theta_{14}\sin\theta_{34}$, we do not need to vary θ_{14} in addition to θ_{34} and θ_{24}.

$$+ 4 \sin\theta_{14} \sin\theta_{24} \sin\theta_{13} \sin\theta_{23} \sin\left(\frac{\Delta m_{31}^2 L}{4E}\right) \sin\left(\frac{\Delta m_{31}^2 L}{4E} \pm \phi_{13} \mp \phi_{14}\right)$$

$$\pm 4LV_{cc}\sin^2\theta_{13}\sin^2\theta_{23}\left\{\frac{4E}{\Delta m_{31}^2 L}\sin^2\left(\frac{\Delta m_{31}^2 L}{4E}\right) - \frac{1}{2}\sin\left(\frac{\Delta m_{31}^2 L}{2E}\right)\right\}$$

$$\pm \sin\theta_{13} \sin\theta_{23} \sin(2\theta_{23}) \sin\theta_{14} \sin\theta_{34} LV_{nc} \cdot F\left(\frac{L\Delta m_{31}^2}{4E}, \pm(\phi_{13} - \phi_{14} + \phi_{34})\right)$$

$$= 4\sin^2\theta_{13}\sin^2\theta_{23}\sin^2\left(\frac{\Delta m_{31}^2 L}{4E}\right) \tag{3}$$

$$+ \{\mp A \sin\phi_{13} + B \cos(\phi_{13} - \phi_{14})\}\sin^2\left(\frac{\Delta m_{31}^2 L}{4E}\right) \tag{4}$$

$$+ \frac{1}{2}\{A \cos\phi_{13} \pm B \sin(\phi_{13} - \phi_{14})\} \sin\left(\frac{\Delta m_{31}^2 L}{2E}\right) \tag{5}$$

$$\pm 4LV_{cc}\sin^2\theta_{13}\sin^2\theta_{23}\left\{\frac{4E}{\Delta m_{31}^2 L}\sin^2\left(\frac{\Delta m_{31}^2 L}{4E}\right) - \frac{1}{2}\sin\left(\frac{\Delta m_{31}^2 L}{2E}\right)\right\} \tag{6}$$

$$\pm \sin\theta_{13} \sin\theta_{23} \sin(2\theta_{23}) \sin\theta_{14} \sin\theta_{34} LV_{nc} \cdot F\left(\frac{L\Delta m_{31}^2}{4E}, \pm(\phi_{13} - \phi_{14} + \phi_{34})\right), \tag{7}$$

where

$$A = 4 \sin\theta_{13} \sin\theta_{12} \cos\theta_{12} \sin(2\theta_{23})\frac{\Delta m_{21}^2 L}{4E},$$
$$B = 4 \sin\theta_{14} \sin\theta_{24} \sin\theta_{13} \sin\theta_{23}, \tag{8}$$

and the upper signs in $\pm$, $\mp$ refer to the neutrino oscillation, and the lower signs to the antineutrino oscillation.

First, we find that in the absence of sterile-active mixings, we have $B = 0$ and the impact of A on the θ_{23} octant measurement can be reduced by a combination of neutrino- and antineutrino-focusing beams, since A term in Eq. (4) changes sign for neutrino and antineutrino.

Second, we observe that in the presence of sterile-active mixings (i.e., $B \neq 0$), a combination of neutrino- and antineutrino-focusing beams *and* two different baseline lengths revives the sensitivity to the θ_{23} octant, because a different oscillating function, $\sin(\Delta m_{31}^2 L/(2E))$, enters Eq. (5). In the rest of the paper, we will confirm this qualitative observation through simulations of T2HK, T2HKK, and T2HK + Oki experiments.

The term Eq. (6) represents the ordinary matter effect that is present in the standard oscillations and does not affect the measurement of the θ_{23} octant.

The last term Eq. (7) represents a synergy of the matter effect and sterile-active mixings. Here, F is a complicated function of $L\Delta m_{31}^2/(4E)$ and $\pm(\phi_{13} - \phi_{14} + \phi_{34})$ and is expected to be $O(1)$. Since θ_{34} is less constrained than θ_{24},

this term can lead to interesting phenomenology in some long baseline experiments with large matter effect. We will study the impact of the term Eq. (7) numerically in the next section.

III. NUMERICAL STUDY

We simulate the propagation of neutrinos and antineutrinos, their 3 + 1 oscillations, and their measurements at Kamioka, Oki, and Korea. We calculate $\nu_\mu \to \nu_e$, $\bar{\nu}_\mu \to \bar{\nu}_e$, $\nu_\mu \to \nu_\mu$, $\bar{\nu}_\mu \to \bar{\nu}_\mu$ oscillation probabilities using Eq. (2) without approximation.

A. Oscillation parameters

We make a simplifying assumption that θ_{12}, θ_{13}, Δm_{21}^2, $|\Delta m_{32}^2|$, and the true mass hierarchy have been measured precisely prior to a θ_{23} measurement. Accordingly, we fix the values of θ_{12}, θ_{13}, Δm_{21}^2, $|\Delta m_{32}^2|$ at their Particle Data Group values [41] in the simulation and fit the simulation results with the true values. Likewise, we perform the simulation for the normal hierarchy case ($\Delta m_{32}^2 > 0$) and fit the results by assuming the normal hierarchy and do this analogously for the inverted hierarchy case ($\Delta m_{32}^2 < 0$).

For sterile-active mixing parameters, we consider a situation, where sterile-active mixings have already been discovered and Δm_{41}^2, θ_{14}, θ_{24}, θ_{34} have been measured precisely in short baseline experiments.

The full analysis is multidimensional, depending on benchmark values of θ_{14}, θ_{24}, θ_{34} as well as unknown

TABLE I. Parameters in the first benchmark.

Parameter	Value in our simulation
$\sin^2 \theta_{12}$	0.304
$\sin^2 \theta_{13}$	0.0219
$\sin^2 \theta_{23}$	0.44 or 0.60
ϕ_{13} (rad)	$[0, 2\pi]$
Δm_{21}^2	7.53×10^{-5} eV^2
Δm_{32}^2 (normal hierarchy)	2.51×10^{-3} eV^2
Δm_{32}^2 (inverted hierarchy)	-2.56×10^{-3} eV^2
$\sin^2 \theta_{14}$	0.04
$\sin^2 \theta_{24}$	0.006
$\sin^2 \theta_{34}$	0
ϕ_{14} (rad)	$[0, 2\pi]$
ϕ_{34} (rad)	unphysical
Δm_{41}^2	3 eV^2

TABLE II. Parameters in the second benchmark. The values of ϕ_{13}, ϕ_{14} are such that sterile-active mixings most afflict the θ_{23} octant measurement in the first benchmark Table I, where $\sin^2 \theta_{34} = 0$.

Parameter	Value in our simulation
$\sin^2 \theta_{12}$	0.304
$\sin^2 \theta_{13}$	0.0219
$\sin^2 \theta_{23}$	0.44 or 0.60
ϕ_{13} (rad)	0 when $\sin^2 \theta_{23} = 0.44$, π when $\sin^2 \theta_{23} = 0.60$
Δm_{21}^2	7.53×10^{-5} eV^2
Δm_{32}^2 (normal hierarchy)	2.51×10^{-3} eV^2
Δm_{32}^2 (inverted hierarchy)	-2.56×10^{-3} eV^2
$\sin^2 \theta_{14}$	0.04
$\sin^2 \theta_{24}$	0.006
$\sin^2 \theta_{34}$	$[0, 0.18]$
ϕ_{14} (rad)	0
ϕ_{34} (rad)	$[0, 2\pi]$
Δm_{41}^2	3 eV^2

values of θ_{23} and the three CP phases $\phi_{13}, \phi_{14}, \phi_{34}$. Such a complicated analysis does not provide clear physical insight. Therefore, first, we restrict our study to the case with $\theta_{34} = 0$ and assume the largest values for θ_{14}, θ_{24} that are consistent with the current experimental bounds in order to *assess the maximal impact of θ_{14}, θ_{24} mixings on the θ_{23} octant measurement*. The reason for taking $\theta_{34} = 0$ is that the θ_{34} mixing affects the octant measurement only via the matter effect, and so its impact should be studied separately. Here, we fix Δm_{41}^2 at a value around ~ 1 eV^2, since the results do not depend on the precise value of Δm_{41}^2. In contrast, we consider various values for ϕ_{13}, ϕ_{14} because the impact of θ_{14}, θ_{24} mixings on the θ_{23} octant measurement depends keenly on ϕ_{13}, ϕ_{14}. We take two benchmark values for θ_{23}, one in the lower octant and the other in the higher octant. The first benchmark parameter set, which is motivated by the above argument, is presented in Table I.

In Table I, the values of $\sin^2 \theta_{14}$ and Δm_{41}^2 are marginally compatible with the 90% C.L. bound obtained by a reanalysis [42] of Bugey-3 [43] experiment, and the values of $\sin^2 \theta_{24}$ and Δm_{41}^2 are marginally consistent with the 90% C.L. bound of the MINOS and MINOS+ results [44] and are outside the 90% C.L. bound from the IceCube [45]. The asymmetric benchmark values of $\sin^2 \theta_{23}$ are motivated by the 3σ range reported by NuFIT 4.1 [46,47], which is tilted towards the higher octant region. Note that ϕ_{34} is an unphysical phase when $\theta_{34} = 0$.

After the analysis of the first benchmark Table I, we vary $\sin^2 \theta_{34}, \phi_{34}$ and study the impact of a synergy of the matter effect and sterile-active mixings described by Eq. (7). Here, we fix ϕ_{13}, ϕ_{14} at the values for which sterile-active mixings have most afflicted the θ_{23} octant measurement in the first benchmark. The second benchmark parameter set, which is motivated by the above argument, is presented in Table II.

In Table II, the range of $\sin^2 \theta_{34}$ is chosen to satisfy the 90% C.L. bound on the sterile-tau neutrino mixing reported

from super-Kamiokande atmospheric neutrino measurement [48].

We will find in Sec. III E that nonzero values of $\sin^2 \theta_{34}$ tend to mitigate the impact of sterile-active mixings on the θ_{23} octant measurement; i.e., one is more likely to obtain the correct octant when the θ_{34} mixing is present. Therefore, it is important to study how the impact of sterile-active mixings changes with θ_{14}, θ_{24} in the "worst scenario" for the octant measurement where $\theta_{34} = 0$. To this end, we vary θ_{24} while fixing $\theta_{34} = 0$. Here, we fix $\sin^2 \theta_{14} = 0.04$ because, as seen in Eqs. (3)–(7), the effects of sterile-active mixings on the θ_{23} octant measurement appear only in the combination $\sin \theta_{14} \sin \theta_{24}$ when $\theta_{34} = 0$, and thus, varying $\sin^2 \theta_{14}$ is equivalent to varying $\sin^2 \theta_{24}$. Here, we take a specific combination of values of ϕ_{13}, ϕ_{14} for which sterile-active mixings have most afflicted the θ_{23} octant measurement in the first benchmark. The third benchmark parameter set, which is motivated by the above argument, is presented in Table III.

B. Experiments

We assume that J-PARC operates with 1.3 MW beam power, delivering 2.7×10^{21} proton-on-target (POT) flux per year. We adopt the values in Table IV as the baseline and detector parameters, where the matter density is approximated to be uniform [49,50]. We consider three experiments, referred to as "T2HK," "T2HKK," and "T2HK + Oki," in this paper. The configuration of each experiment is assumed as follows and is summarized in Table IV.

(i) In "T2HK," we assume that one 187 kton fiducial volume detector at Kamioka is exposed to a neutrino-focusing beam for 2.5 yr and to an antineutrino-focusing beam for 2.5 yr. Subsequently, two

TABLE III. Parameters in the third benchmark. The values of ϕ_{13}, ϕ_{14} are such that sterile-active mixings most afflict the θ_{23} octant measurement in the first benchmark Table I, where we fix $\sin^2\theta_{24} = 0.006$.

Parameter	Value in our simulation
$\sin^2\theta_{12}$	0.304
$\sin^2\theta_{13}$	0.0219
$\sin^2\theta_{23}$	0.44 or 0.60
ϕ_{13} (rad)	$[0, 2\pi]$
Δm_{21}^2	7.53×10^{-5} eV^2
Δm_{32}^2 (normal hierarchy)	2.51×10^{-3} eV^2
Δm_{32}^2 (inverted hierarchy)	-2.56×10^{-3} eV^2
$\sin^2\theta_{14}$	0.04
$\sin^2\theta_{24}$	$[0, 0.006]$
$\sin^2\theta_{34}$	0
ϕ_{14} (rad)	equals ϕ_{13} when $\sin^2\theta_{23} = 0.44$, equals $\phi_{13} + \pi$ when $\sin^2\theta_{23} = 0.60$
ϕ_{34} (rad)	unphysical
Δm_{41}^2	3 eV^2

187 kton detectors (374 kton in total) at Kamioka are exposed to a neutrino-focusing beam for 5 yr and to an antineutrino-focusing beam for 5 yr.

(ii) In "T2HKK," we assume that one 187 kton detector at Kamioka is exposed to a neutrino-focusing beam for 2.5 yr and to an antineutrino-focusing beam for 2.5 yr. Subsequently, one 187 kton detector at Kamioka and one 187 kton detector in Korea are exposed to a neutrino-focusing beam for 5 yr and to an antineutrino-focusing beam for 5 yr.

(iii) In 'T2HK + Oki', we assume that one 187 kton detector at Kamioka is exposed to a neutrino-focusing beam for 2.5 yr and to an antineutrino-focusing beam for 2.5 yr. Subsequently, one 187 kton detector at Kamioka and a smaller 100 kton detector at Oki Islands are exposed to a neutrino-focusing beam for 5 yr and to an antineutrino-focusing beam for 5 yr.

C. Number of events

The number of $\nu_e + \bar{\nu}_e$ events and the number of $\nu_\mu + \bar{\nu}_\mu$ events in the bin of $0.4 + (i-1) \cdot 0.05$ GeV $< E < 0.4 + i \cdot 0.05$ GeV with a neutrino-focusing beam that are detected at a specific site, denoted by $N_{e,i,\text{site}}$ and $N_{\mu,i,\text{site}}$, and those with an antineutrino-focusing beam, denoted by $\tilde{N}_{e,i,\text{site}}$ and $\tilde{N}_{\mu,i,\text{site}}$, are computed as

For $i = 1, 2, 3, \ldots, 52$,

$$N_{e,i,\text{site}} = \int_{0.4+(i-1)\cdot 0.05\,\text{GeV}}^{0.4+i\cdot 0.05\,\text{GeV}} dE\, \varepsilon_{e,\text{site}} f_{\sigma e} \{ f_{\Phi_\nu} \Phi_{\nu,\text{site}}(E) P_{\text{site}}(\nu_\mu \to \nu_e; E) N_{n,\text{site}} \sigma(\nu_\ell n \to \ell^- p; E)$$
$$+ f_{\Phi_{\bar{\nu}}} \Phi_{\bar{\nu},\text{site}}(E) P_{\text{site}}(\bar{\nu}_\mu \to \bar{\nu}_e; E) N_{p,\text{site}} \sigma(\bar{\nu}_\ell p \to \ell^+ n; E) \}, \tag{9}$$

$$N_{\mu,i,\text{site}} = \int_{0.4+(i-1)\cdot 0.05\,\text{GeV}}^{0.4+i\cdot 0.05\,\text{GeV}} dE\, \varepsilon_{\mu,\text{site}} f_{\sigma\mu} \{ f_{\Phi_\nu} \Phi_{\nu,\text{site}}(E) P_{\text{site}}(\nu_\mu \to \nu_\mu; E) N_{n,\text{site}} \sigma(\nu_\ell n \to \ell^- p; E)$$
$$+ f_{\Phi_{\bar{\nu}}} \Phi_{\bar{\nu},\text{site}}(E) P_{\text{site}}(\bar{\nu}_\mu \to \bar{\nu}_\mu; E) N_{p,\text{site}} \sigma(\bar{\nu}_\ell p \to \ell^+ n; E) \},$$

$$\tilde{N}_{e,i,\text{site}} = \text{replace}(\Phi_{\nu,\text{site}}(E), \Phi_{\bar{\nu},\text{site}}(E), \varepsilon_{e,\text{site}}, f_{\Phi_\nu}, f_{\Phi_{\bar{\nu}}}, f_{\sigma e}) \text{in } N_{e,i,\text{site}}$$
$$\text{with} \quad (\tilde{\Phi}_{\nu,\text{site}}(E), \tilde{\Phi}_{\bar{\nu},\text{site}}(E), \tilde{\varepsilon}_{e,\text{site}}, \tilde{f}_{\Phi_\nu}, \tilde{f}_{\Phi_{\bar{\nu}}}, \tilde{f}_{\sigma e})$$

$$\tilde{N}_{\mu,i,\text{site}} = \text{replace}(\Phi_{\nu,\text{site}}(E), \Phi_{\bar{\nu},\text{site}}(E), \varepsilon_{\mu,\text{site}}, f_{\Phi_\nu}, f_{\Phi_{\bar{\nu}}}, f_{\sigma\mu}) \text{in } N_{\mu,i,\text{site}}$$
$$\text{with} \quad (\tilde{\Phi}_{\nu,\text{site}}(E), \tilde{\Phi}_{\bar{\nu},\text{site}}(E), \tilde{\varepsilon}_{\mu,\text{site}}, \tilde{f}_{\Phi_\nu}, \tilde{f}_{\Phi_{\bar{\nu}}}, \tilde{f}_{\sigma\mu}), \tag{10}$$

TABLE IV. Baseline and detector parameters. L, FV, ρ, "off axis," "ν focusing," and "$\bar{\nu}$ focusing" denote the baseline length, the fiducial volume, matter density, off axis angle, the time of exposure to a neutrino-focusing beam, and that to an antineutrino-focusing beam, respectively.

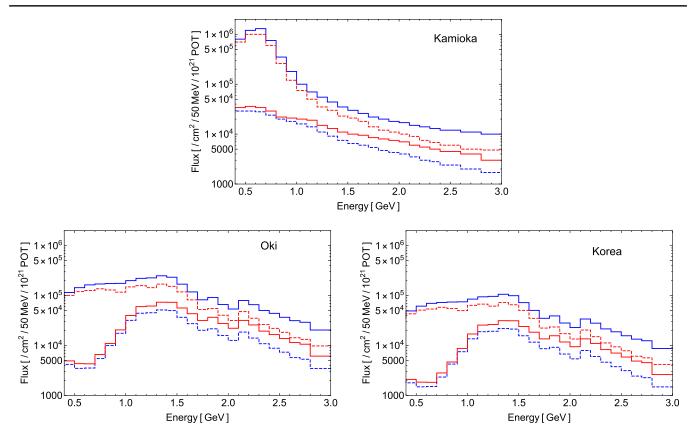| Experiment	Site	L	FV	ρ	Off axis	ν focusing	$\bar{\nu}$ focusing
T2HK	Kamioka	295 km	187 kton	2.60 g/cm^3	2.5°	2.5 yr	2.5 yr
	Kamioka	295 km	374 kton	2.60 g/cm^3	2.5°	5 yr	5 yr
T2HKK	Kamioka	295 km	187 kton	2.60 g/cm^3	2.5°	2.5 yr	2.5 yr
	Kamioka	295 km	187 kton	2.60 g/cm^3	2.5°	5 yr	5 yr
	Korea	1000 km	187 kton	2.90 g/cm^3	1.0°	5 yr	5 yr
T2HK + Oki	Kamioka	295 km	187 kton	2.60 g/cm^3	2.5°	2.5 yr	2.5 yr
	Kamioka	295 km	187 kton	2.60 g/cm^3	2.5°	5 yr	5 yr
	Oki	653 km	100 kton	2.75 g/cm^3	1.0°	5 yr	5 yr

FIG. 1.   Flux of ν_μ and $\bar{\nu}_\mu$ in neutrino-focusing and antineutrino-focusing beams detected at a water Cerenkov detector at Kamioka, Oki, and in Korea if the neutrino oscillations were absent, taken from Ref. [51]. The baseline length and beam off axis angle of each detector are as given in Table IV. The upper plot, the lower-left plot, and the lower-right plot correspond to Kamioka, Oki, and Korea, respectively. In the plots, the blue lines correspond to a neutrino-focusing beam and the red lines to an antineutrino-focusing beam. The solid lines indicate ν_μ flux and the dashed lines $\bar{\nu}_\mu$ flux.

where $\Phi_{\nu,\mathrm{site}}(E)$, $\Phi_{\bar{\nu},\mathrm{site}}(E)$ [$\tilde{\Phi}_{\nu,\mathrm{site}}(E)$, $\tilde{\Phi}_{\bar{\nu},\mathrm{site}}(E)$], respectively, denote ν_μ and $\bar{\nu}_\mu$ fluxes per energy in a neutrino-focusing beam (in an antineutrino-focusing beam) at a specific detector. P_{site} denotes a transition probability calculated with Eq. (2) for a specific site. $N_{n,\mathrm{site}}$ and $N_{p,\mathrm{site}}$ are, respectively, the number of neutrons and protons in the water Cerenkov detector at a specific site. σ denotes the cross sections for the $\nu_\ell n \to \ell^- p$ and $\bar{\nu}_\ell p \to \ell^+ n$ processes.

We employ the result of Ref. [51] for ν_μ and $\bar{\nu}_\mu$ flux in neutrino-focusing and antineutrino-focusing beams emitted from J-PARC and detected at a water Cerenkov detector at Kamioka, Oki, and in Korea if the neutrino oscillations were absent. For reference, we plot the flux in Fig. 1. The baseline length and beam off axis angle of each detector are found in Table IV. In the plots, the blue lines correspond to a neutrino-focusing beam and the red lines to an antineutrino-focusing beam. The solid lines indicate ν_μ flux and the dashed lines $\bar{\nu}_\mu$ flux.

ν_e and $\bar{\nu}_e$ components in the beams are neglected in our study.

The cross sections for charged current quasielastic scattering between a neutrino and a proton, $\nu_\ell n \to \ell^- p$,

and that between an antineutrino and a neutron, $\bar{\nu}_\ell p \to \ell^+ n$, ($p$ and n denote proton and neutron, respectively, and ℓ denotes e or μ) are obtained from Ref. [52].

$\varepsilon_{e,\mathrm{site}}$, $\varepsilon_{\mu,\mathrm{site}}$, respectively, denote the efficiencies for electrons and muons of the far detector at a specific site, in a neutrino-focusing run. f_{Φ_ν}, $f_{\Phi_{\bar{\nu}}}$ account for the uncertainty of neutrino and antineutrino fluxes, respectively, in a neutrino-focusing beam. $f_{\sigma e}$ ($f_{\sigma\mu}$) accounts for the uncertainty of the weighted sum of charged current quasielastic scattering cross sections of ν_e and $\bar{\nu}_e$ (ν_μ and $\bar{\nu}_\mu$) that is estimated from near detector data and theory in a neutrino-focusing run. $\tilde{\varepsilon}_{e,\mathrm{site}}$, $\tilde{\varepsilon}_{\mu,\mathrm{site}}$, $\tilde{f}_{\Phi_\nu}$, $\tilde{f}_{\Phi_{\bar{\nu}}}$, $\tilde{f}_{\sigma e}$, $\tilde{f}_{\sigma\mu}$ are the corresponding quantities in an antineutrino-focusing run. In this paper, we neglect energy dependence of the above systematic parameters. For the efficiencies of the far detectors, based on Table 9 of Ref. [53], we assume[3]

---

[3]We consider that the same water Cerenkov detector as Kamioka is situated at Oki.

$$\varepsilon_{e,\text{site}} = 1 \pm 0.007, \qquad \varepsilon_{\mu,\text{site}} = 1 \pm 0.010, \qquad \tilde{\varepsilon}_{e,\text{site}} = 1 \pm 0.017, \qquad \tilde{\varepsilon}_{\mu,\text{site}} = 1 \pm 0.011.$$

$$\varepsilon_{e,\text{site}} \text{ and } \tilde{\varepsilon}_{e,\text{site}} \text{ at each site are maximally correlated.}$$

$$\varepsilon_{\mu,\text{site}} \text{ and } \tilde{\varepsilon}_{\mu,\text{site}} \text{ at each site are maximally correlated.} \tag{11}$$

For the flux uncertainty, based on Fig. 9 of Ref. [53], we approximate

$$f_{\Phi_\nu} = 1 \pm 0.1, \qquad f_{\Phi_{\bar{\nu}}} = 1 \pm 0.08, \qquad \tilde{f}_{\Phi_\nu} = 1 \pm 0.1, \qquad \tilde{f}_{\Phi_{\bar{\nu}}} = 1 \pm 0.1. \tag{12}$$

For the cross section uncertainty, based on Table 9 of Ref. [53], we assume

$$f_{\sigma e} = 1 \pm \sqrt{0.030^2 + 0.012^2}, \qquad f_{\sigma\mu} = 1 \pm \sqrt{0.028^2 + 0.015^2},$$
$$\tilde{f}_{\sigma e} = 1 \pm \sqrt{0.056^2 + 0.020^2}, \qquad \tilde{f}_{\sigma\mu} = 1 \pm \sqrt{0.042^2 + 0.014^2}. \tag{13}$$

All uncertainties above are assumed to be uncorrelated unless otherwise stated.

D. χ^2 analysis

We perform a χ^2 fit of the numbers of events in the bins with neutrino-focusing and antineutrino-focusing beams measured at Kamioka/Korea/Oki, $N_{e,i,\text{site}}$, $N_{\mu,i,\text{site}}$, $\tilde{N}_{e,i,\text{site}}$, and $\tilde{N}_{\mu,i,\text{site}}$ ($i = 1, 2, \ldots, 52$; site = Kamioka, Korea, Oki). In the fitting analysis, we vary $\sin^2\theta_{23}$, ϕ_{13}, ϕ_{14}, and ϕ_{34} freely, while using true values for the other standard mixing angles θ_{12}, θ_{13}, the sterile-active mixing angles θ_{14}, θ_{24}, θ_{34}, and the mass differences Δm_{21}^2, $|\Delta m_{32}^2|$, Δm_{41}^2. Such an analysis is justifiable because θ_{12}, θ_{13}, θ_{14}, θ_{24}, θ_{34}, Δm_{21}^2, $|\Delta m_{32}^2|$, Δm_{41}^2 can be measured to a good accuracy in short baseline experiments and atmospheric neutrino measurements, while the octant of θ_{23} and the CP phases ϕ_{13}, ϕ_{14}, ϕ_{34} can be measured precisely only in long

baseline experiments. Additionally, we fit the normal hierarchy events by assuming the normal hierarchy, and the inverted hierarchy events by assuming the inverted hierarchy, because the mass hierarchy may have been determined before T2HK starts operation.

We take into account the uncertainties of the efficiencies of far detectors $\varepsilon_{e,\text{site}}$, $\varepsilon_{\mu,\text{site}}$, $\tilde{\varepsilon}_{e,\text{site}}$, $\tilde{\varepsilon}_{\mu,\text{site}}$, those of neutrino-focusing and antineutrino-focusing beam fluxes f_{Φ_ν}, $f_{\Phi_{\bar{\nu}}}$, $\tilde{f}_{\Phi_\nu}$, $\tilde{f}_{\Phi_{\bar{\nu}}}$, and those of the cross sections (estimated from near detector data and theory) $f_{\sigma e}$, $f_{\sigma\mu}$, $\tilde{f}_{\sigma e}$, $\tilde{f}_{\sigma\mu}$, which constitute systematic uncertainties. We vary the above parameters, with the inclusion of the maximal correlation of $\varepsilon_{e,\text{site}}$ and $\tilde{\varepsilon}_{e,\text{site}}$, and that of $\varepsilon_{\mu,\text{site}}$ and $\tilde{\varepsilon}_{\mu,\text{site}}$. Eventually, the χ^2 function is given by

$$\chi^2(\sin^2\theta_{23}, \phi_{13}, \phi_{14}, \phi_{34}, \Pi_{\text{sys}}) = \sum_{\text{site}} \sum_{i=1}^{52}$$

$$\left[\frac{(N_{e,i,\text{site}} - N_{e,i,\text{site}}^{\text{pred}}(\sin^2\theta_{23}, \phi_{13}, \phi_{14}, \phi_{34}, \Pi_{\text{sys}}))^2}{N_{e,i,\text{site}}} + \frac{(N_{\mu,i,\text{site}} - N_{\mu,i,\text{site}}^{\text{pred}}(\sin^2\theta_{23}, \phi_{13}, \phi_{14}, \phi_{34}, \Pi_{\text{sys}}))^2}{N_{\mu,i,\text{site}}} \right.$$

$$\left. + \frac{(\tilde{N}_{e,i,\text{site}} - \tilde{N}_{e,i,\text{site}}^{\text{pred}}(\sin^2\theta_{23}, \phi_{13}, \phi_{14}, \phi_{34}, \Pi_{\text{sys}}))^2}{\tilde{N}_{e,i,\text{site}}} + \frac{(\tilde{N}_{\mu,i,\text{site}} - \tilde{N}_{\mu,i,\text{site}}^{\text{pred}}(\sin^2\theta_{23}, \phi_{13}, \phi_{14}, \phi_{34}, \Pi_{\text{sys}}))^2}{\tilde{N}_{\mu,i,\text{site}}} \right]$$

$$+ \sum_{\text{site}} \left\{ \left(\frac{\varepsilon_{e,\text{site}} - 1}{0.007} \right)^2 + \left(\frac{\varepsilon_{\mu,\text{site}} - 1}{0.010} \right)^2 \right\} + \left(\frac{f_{\Phi_\nu} - 1}{0.1} \right)^2 + \left(\frac{f_{\Phi_{\bar{\nu}}} - 1}{0.08} \right)^2 + \left(\frac{\tilde{f}_{\Phi_\nu} - 1}{0.1} \right)^2 + \left(\frac{\tilde{f}_{\Phi_{\bar{\nu}}} - 1}{0.1} \right)^2$$

$$+ \left(\frac{f_{\sigma e} - 1}{0.032} \right)^2 + \left(\frac{f_{\sigma\mu} - 1}{0.032} \right)^2 + \left(\frac{\tilde{f}_{\sigma e} - 1}{0.059} \right)^2 + \left(\frac{\tilde{f}_{\sigma\mu} - 1}{0.044} \right)^2 \tag{14}$$

where $\Pi_{\text{sys}} = \{\varepsilon_{e,\text{site}}, \varepsilon_{\mu,\text{site}}, f_{\Phi_\nu}, f_{\Phi_{\bar{\nu}}}, \tilde{f}_{\Phi_\nu}, \tilde{f}_{\Phi_{\bar{\nu}}}, f_{\sigma e}, f_{\sigma\mu}, \tilde{f}_{\sigma e}, \tilde{f}_{\sigma\mu}\}$

and $\quad \tilde{\varepsilon}_{e,\text{site}} - 1 = \dfrac{0.017}{0.007}(\varepsilon_{e,\text{site}} - 1), \qquad \tilde{\varepsilon}_{\mu,\text{site}} - 1 = \dfrac{0.011}{0.010}(\varepsilon_{\mu,\text{site}} - 1). \tag{15}$
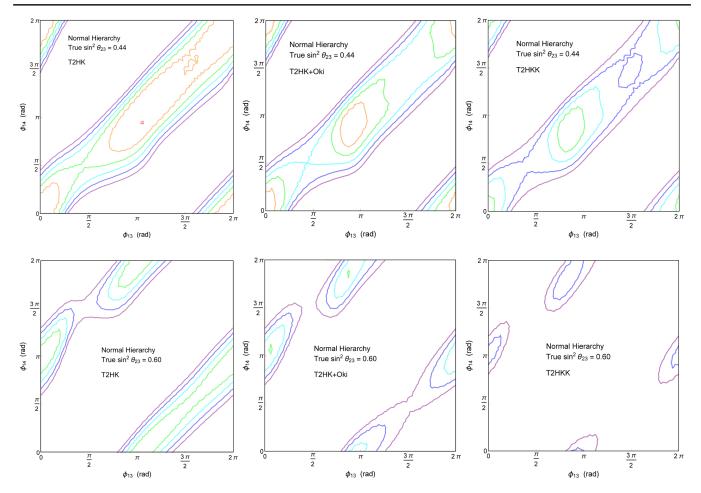
FIG. 2. Significance of rejecting the wrong θ_{23} octant when the true $\sin^2\theta_{23}$ is 0.44, Eq. (16) (upper three panels), and that when the true $\sin^2\theta_{23}$ is 0.60, Eq. (17) (lower three panels), in T2HK, T2HKK, and T2HK + Oki experiments, in the first benchmark Table I. The mass hierarchy is normal. The red, orange, green, cyan, blue, and purple contours correspond to $\Delta\chi^2 = 1^2$, 1.5^2, 2^2, 2.5^2, 3^2, 3.5^2, respectively.

Here, $N_{e,i,\text{site}}$, $N_{\mu,i,\text{site}}$, $\tilde{N}_{e,i,\text{site}}$, and $\tilde{N}_{\mu,i,\text{site}}$ are calculated for the central values of Eqs. (11),(12),(13). $N^{\text{pred}}(\sin^2\theta_{23}, \phi_{13}, \phi_{14}, \phi_{34}, \Pi_{\text{sys}})$ denotes the number of events calculated as a function of $\sin^2\theta_{23}$, ϕ_{13}, ϕ_{14}, ϕ_{34}, and the systematic parameters $\Pi_{\text{sys}} = \{\varepsilon_{e,\text{site}}, \varepsilon_{\mu,\text{site}}, f_{\Phi_\nu}, f_{\Phi_{\bar\nu}}, \tilde{f}_{\Phi_\nu}, \tilde{f}_{\Phi_{\bar\nu}}, f_{\sigma e}, f_{\sigma\mu}, \tilde{f}_{\sigma e}, \tilde{f}_{\sigma\mu}\}$, using the true values of θ_{12}, θ_{13}, Δm^2_{21}, $|\Delta m^2_{32}|$, θ_{14}, θ_{24}, θ_{34}, and the true mass hierarchy. The values of $\tilde{\varepsilon}_{e,\text{site}}$, $\tilde{\varepsilon}_{\mu,\text{site}}$ are calculated from $\varepsilon_{e,\text{site}}$,

$\varepsilon_{\mu,\text{site}}$ through Eq. (15), since they are maximally correlated.

In this paper, we are interested in the danger of wrong measurement of the θ_{23} octant. Thus, we evaluate the significance of rejecting the wrong octant, $\sqrt{\Delta\chi^2}$, which is the square root of the difference between the minimum of χ^2 for $\sin^2\theta_{23} > 1/2$ and that for $\sin^2\theta_{23} < 1/2$. Specifically, for each benchmark with $\sin^2\theta_{23} = 0.44$ or 0.60, $\Delta\chi^2$ is given by

$$\Delta\chi^2 = \min_{\sin^2\theta_{23} > 1/2} \chi^2(\sin^2\theta_{23}, \phi_{13}, \phi_{14}, \phi_{34}, \Pi_{\text{sys}}) - \min_{\sin^2\theta_{23} < 1/2} \chi^2(\sin^2\theta_{23}, \phi_{13}, \phi_{14}, \phi_{34}, \Pi_{\text{sys}})$$

when true $\sin^2\theta_{23}$ is 0.44, $\qquad\qquad\qquad\qquad\qquad\qquad\qquad\qquad\qquad$ (16)

$$\Delta\chi^2 = \min_{\sin^2\theta_{23} < 1/2} \chi^2(\sin^2\theta_{23}, \phi_{13}, \phi_{14}, \phi_{34}, \Pi_{\text{sys}}) - \min_{\sin^2\theta_{23} > 1/2} \chi^2(\sin^2\theta_{23}, \phi_{13}, \phi_{14}, \phi_{34}, \Pi_{\text{sys}})$$

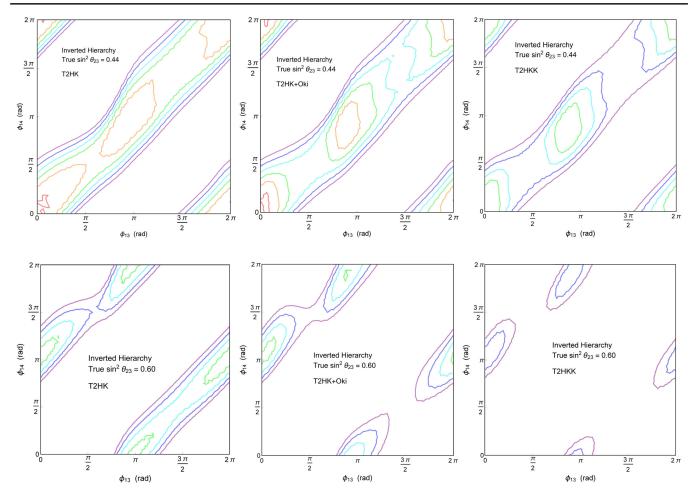when true $\sin^2\theta_{23}$ is 0.60. $\qquad\qquad\qquad\qquad\qquad\qquad\qquad\qquad\qquad$ (17)

FIG. 3. Same as Fig. 2 except that the mass hierarchy is inverted.

We have confirmed that for both $\sin^2 \theta_{23} = 0.44$ and 0.60, the χ^2 function has local minima in both $\sin^2 \theta_{23} > 1/2$ and $\sin^2 \theta_{23} < 1/2$ regions.

E. Results

Before going to the main results, we show in Table V the total numbers of $\nu_\mu + \bar{\nu}_\mu$ events at the Kamioka, Oki, and Korea detectors in T2HK, T2HKK, and T2HK + Oki experiments when there were *no oscillations*, corresponding to the configurations of Table IV and the assumption that J-PARC operates with 1.3 MW beam power.

Now we present $\Delta\chi^2$ with $\sin^2 \theta_{23} = 0.44$ Eq. (16) and that with $\sin^2 \theta_{23} = 0.60$ Eq. (17) in the first benchmark Table I. The results are presented as a function of (ϕ_{13}, ϕ_{14}) and shown separately for the normal and inverted mass hierarchies. Figure 2 is the result when the mass hierarchy is normal, and Fig. 3 is the result when the mass hierarchy is inverted. The red, orange, green, cyan, blue, and purple contours correspond to $\Delta\chi^2 = 1^2,\ 1.5^2,\ 2^2,\ 2.5^2,\ 3^2,\ 3.5^2$, respectively.

The following observations are made from Figs. 2 and 3.

(i) In T2HK, the significance of rejecting the wrong θ_{23} octant can decrease as low as $\sqrt{\Delta\chi^2} < 1.5$ when $\sin^2 \theta_{23} = 0.44$, and as low as $\sqrt{\Delta\chi^2} < 2$ when $\sin^2 \theta_{23} = 0.60$, in a wide region of the (ϕ_{13}, ϕ_{14}) space for both mass hierarchies. This corroborates the claim of Ref. [16].

(ii) In T2HK, when $\sin^2 \theta_{23} = 0.44$, the decrease of the significance is most prominent for $\phi_{13} \simeq \phi_{14}$, and in particular for $(\phi_{13}, \phi_{14}) = (0, 0), (\pi, \pi)$. When $\sin^2 \theta_{23} = 0.60$, the decrease of the significance is most prominent for $\phi_{13} \simeq \phi_{14} + \pi$, and in particular for $(\phi_{13}, \phi_{14}) = (0, \pi), (\pi, 0)$. The above results are quite consistent with Eqs. (3),(4).[4] Since $B \geq 0$ in our phase definition, the second part of Eq. (4) is positively maximal when $\phi_{13} \simeq \phi_{14}$ and is

---

[4]The term Eq. (5) is small around the energy peak at the Kamioka detector and so plays no role in the following argument.
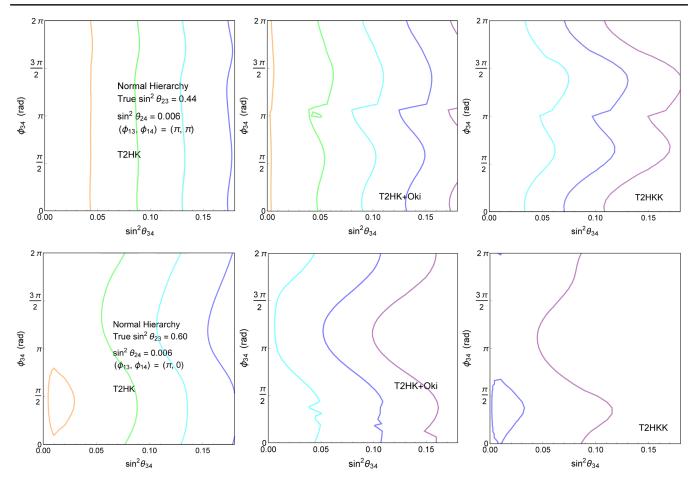
FIG. 4. Significance of rejecting the wrong θ_{23} octant when the true $\sin^2\theta_{23}$ is 0.44, Eq. (16) (upper three panels), and that when the true $\sin^2\theta_{23}$ is 0.60, Eq. (17) (lower three panels), in T2HK, T2HKK, and T2HK + Oki experiments, in the second benchmark Table II. The mass hierarchy is normal. The orange, green, cyan, blue, and purple contours correspond to $\Delta\chi^2 = 1.5^2$, 2^2, 2.5^2, 3^2, 3.5^2, respectively.

negatively maximal when $\phi_{13} \simeq \phi_{14} + \pi$. Hence, this part is most likely to lead to wrong θ_{23} octant measurement when $\sin^2\theta_{23} < 1/2$ and $\phi_{13} \simeq \phi_{14}$, and when $\sin^2\theta_{23} > 1/2$ and $\phi_{13} \simeq \phi_{14} + \pi$. Moreover, when $\phi_{13} = 0, \pi$, the first part of Eq. (4) vanishes, and thus, the combination of neutrino and antineutrino oscillations cannot resolve the above degeneracy.

(iii) T2HKK and T2HK + Oki give a larger significance of rejecting the wrong θ_{23} octant than T2HK in all cases, in spite of their smaller statistics than T2HK (see Table V). This confirms the qualitative argument of Sec. II of the present paper.

(iv) Comparing T2HKK and T2HK + Oki, we observe that T2HKK gives a larger significance, in spite of the fact that T2HKK has smaller statistics than T2HK + Oki (see Table V). The reason that T2HK + Oki, in spite of its larger statistics, shows a smaller improvement of the octant sensitivity than T2HKK is understood as follows: As shown in

Fig. 1, under our assumption that the beam off axis angle at Oki is 1.0°, the flux at Oki has a (broad) peak around $E \simeq 1.4$ GeV. Thus, the value of L/E at the flux peak is 653 km/1.4 GeV for Oki, and it is 295 km/0.6 GeV for Kamioka. Since

TABLE V. The total number of $\nu_\mu + \bar{\nu}_\mu$ events at each detector in each experiment when there were *no oscillations*, corresponding to the configurations of Table IV and J-PARC operation with 1.3 MW beam power.

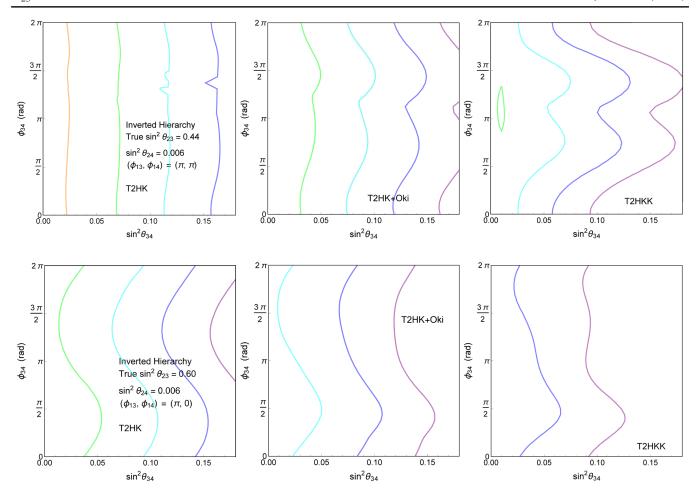| Experiment	Detector	Event number with neutrino-focusing beam ($\times 10^4$)	Event number with antineutrino-focusing beam ($\times 10^4$)
T2HK	Kamioka	13	4.7
T2HKK	Kamioka	7.9	2.8
	Korea	1.6	0.86
T2HK+Oki	Kamioka	7.9	2.8
	Oki	2.0	1.1

FIG. 5.   Same as Fig. 4 except that the mass hierarchy is inverted.

653 km/1.4 GeV and 295 km/0.6 GeV are close values, a major portion of (anti)neutrinos oscillate in a similar manner at Oki and Kamioka, which spoils our attempt to resolve the degeneracy between Eq. (3) and Eqs. (4), (5) by combining different baselines.

Next, we present $\Delta\chi^2$ with $\sin^2\theta_{23} = 0.44$ Eq. (16) and that with $\sin^2\theta_{23} = 0.60$ Eq. (17) in the second benchmark Table II. The results are presented as a function of $(\sin^2\theta_{34}, \phi_{34})$ and shown separately for the normal and inverted mass hierarchies. Figure 4 is the result when the mass hierarchy is normal, and Fig. 5 is the result when the mass hierarchy is inverted.

The following observations are made from Figs. 4 and 5.

(i) T2HKK and T2HK + Oki give a larger significance of rejecting the wrong θ_{23} octant than T2HK in all cases. Also, T2HKK shows a larger significance than T2HK + Oki in all cases.

(ii) Nonzero values of θ_{34} tend to increase the significance of rejecting the wrong θ_{23} octant in both

cases with $\sin^2\theta_{23} = 0.44$ and 0.60, for both mass hierarchies, in all the experiments. Interestingly, even though the matter effect is small in T2HK, we still obtain an increase in the significance in T2HK. The above results are because the term Eq. (7) is proportional to $\sin\theta_{23}$ and flips sign for neutrinos and antineutrinos. Hence, a measurement of this term using the combination of neutrino-focusing and antineutrino-focusing operations offers a new probe for the θ_{23} octant.

(iii) In the case with $\sin^2\theta_{23} = 0.60$ and for small $\sin^2\theta_{34}$, there is a tiny parameter region where the significance of rejecting the wrong θ_{23} octant decreases with θ_{34}. The presence of such a region is probably because the term Eq. (7) mimics the first part of Eq. (4) [remember that $\phi_{13} = \pi$ in the second benchmark and so the true value of the first part of Eq. (4) is 0], which makes it harder to distinguish the term Eq. (4) from the term Eq. (3).

Finally, we present $\Delta\chi^2$ with $\sin^2\theta_{23} = 0.44$ Eq. (16) and that with $\sin^2\theta_{23} = 0.60$ Eq. (17) in the third
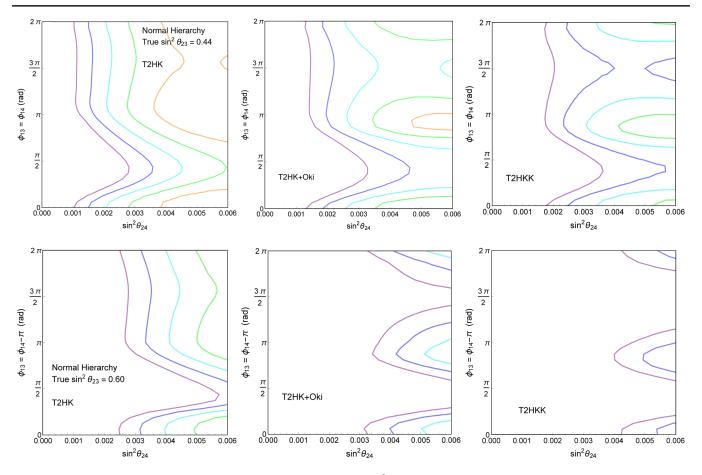
FIG. 6. Significance of rejecting the wrong θ_{23} octant when the true $\sin^2 \theta_{23}$ is 0.44, Eq. (16) (upper three panels), and that when the true $\sin^2 \theta_{23}$ is 0.60, Eq. (17) (lower three panels), in T2HK, T2HKK, and T2HK + Oki experiments, in the third benchmark Table III. The mass hierarchy is normal. The orange, green, cyan, blue, and purple contours correspond to $\Delta\chi^2 = 1.5^2, 2^2, 2.5^2, 3^2, 3.5^2$, respectively.

benchmark Table III. The results are presented as a function of $(\sin^2\theta_{24}, \phi_{13} = \phi_{14})$ for $\sin^2 \theta_{23} = 0.44$ and $(\sin^2\theta_{24}, \phi_{13} = \phi_{14} - \pi)$ for $\sin^2 \theta_{23} = 0.60$ and shown separately for the normal and inverted mass hierarchies. Figure 6 is the result when the mass hierarchy is normal, and Fig. 7 is the result when the mass hierarchy is inverted.

The following observations are made from Figs. 6 and 7.

(i) T2HKK and T2HK + Oki give a larger significance of rejecting the wrong θ_{23} octant than T2HK in all cases. Also, T2HKK shows a larger significance than T2HK + Oki in all cases.

(ii) The significance of rejecting the wrong θ_{23} octant mostly decreases with $\sin^2 \theta_{24}$ in both cases with $\sin^2 \theta_{23} = 0.44$ and 0.60, for both mass hierarchies, in all the experiments. The significance in T2HK is above 3 for $\sin^2 \theta_{24} < 0.0015$ (with $\sin^2 \theta_{14} = 0.004$) when $\sin^2 \theta_{23} = 0.44$, and for $\sin^2 \theta_{24} < 0.003$ (with $\sin^2 \theta_{14} = 0.004$) when $\sin^2 \theta_{23} = 0.60$. This suggests that the sensitivity of T2HK to the θ_{23} octant is

recovered for such small values of sterile-active mixings.

(iii) When $\sin^2 \theta_{23} = 0.44$, for $\phi_{13} \simeq 3\pi/2$ and for large $\sin^2 \theta_{24}$, there is a tiny parameter region where the significance increases with $\sin^2 \theta_{24}$. The presence of such a region is probably because for larger $\sin^2 \theta_{24}$, the first part of Eq. (4) is less likely to mimic the second part of Eq. (5) [remember that $\phi_{13} - \phi_{14} = 0, \pi$ in the third benchmark, and so the true value of the second part of Eq. (5) is zero], which makes it easier to distinguish the first part of Eq. (4) from the other terms. Then the combination of neutrino- and antineutrino-focusing operations can more easily resolve the degeneracy between Eqs. (3) and (4).

We note in passing that in the χ^2 minimum in the wrong octant region, the fitted value of ϕ_{13} is close to its true value. So, even if the sensitivity to the θ_{23} octant is lost, the measurement of the standard CP phase is relatively unaffected.
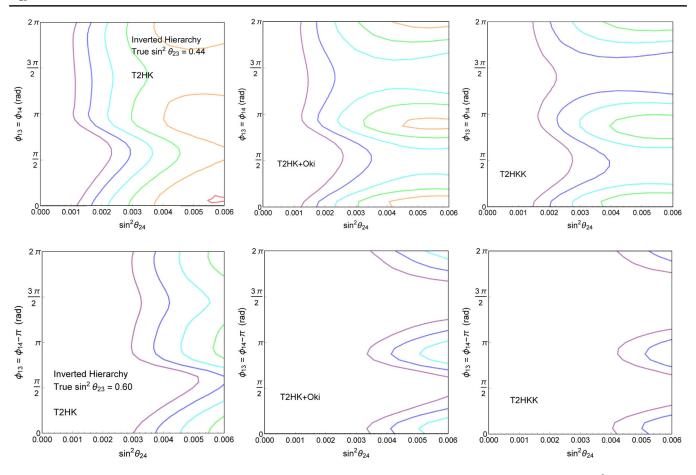
FIG. 7. Same as Fig. 6 except that the mass hierarchy is inverted. The red contour corresponds to $\Delta\chi^2 = 1$.

IV. SUMMARY

We have confirmed that in the presence of sterile-active mixings with nonzero θ_{14} and θ_{24}, T2HK experiment with two 187 kton detectors at Kamioka can lose sensitivity to the θ_{23} octant, depending on values of CP phases. We have revealed that T2HKK exhibits a better sensitivity to the θ_{23} octant in all parameter regions, including those where the experiment with two detectors at Kamioka loses its sensitivity, in spite of the smaller statistics of T2HKK. The better sensitivity of T2HKK is because measurements of the same beam at Kamioka and Korea, which involve distinctively different baseline lengths, resolve the degeneracy between the atmospheric oscillation probability and the sum of the interferences with the solar oscillation amplitude and the active-sterile oscillation amplitude. We have further studied the impact of nonzero θ_{34} mixing and found that the sensitivity to the θ_{23} octant tends to increase with θ_{34} in all parameter regions in all the experiments.

Our results suggest that if a hint of sterile-active mixings with $\theta_{14} \neq 0$ and $\theta_{24} \neq 0$ is discovered but θ_{34} is 0 or substantially smaller than the current experimental bound, T2HKK is a preferable option compared to the plan of placing the two detectors at Kamioka, for the determination of the θ_{23} octant.

Additionally, we have studied a case where one 187 kton detector is at Kamioka and a 100 kton detector is at Oki Islands. This case also shows a better sensitivity to the θ_{23} octant in those parameter regions, where the plan of two 187 kton detectors loses its sensitivity, but the improvement is quite mild compared to T2HKK, in spite of its larger statistics than T2HKK.

[1] P. S. Bhupal Dev, B. Dutta, R. N. Mohapatra, and M. Severson, θ_{13} and proton decay in a minimal $SO(10) \times S_4$ model of flavor, Phys. Rev. D **86,** 035002 (2012).

[2] T. Fukuyama, K. Ichikawa, and Y. Mimura, Revisiting fermion mass and mixing fits in the minimal SUSY $SO(10)$ GUT, Phys. Rev. D **94,** 075018 (2016).

[3] T. Fukuyama, K. Ichikawa, and Y. Mimura, Relation between proton decay and PMNS phase in the minimal SUSY $SO(10)$ GUT, Phys. Lett. B **764,** 114 (2017).

[4] V. Barger, D. Marfatia, and K. Whisnant, Breaking eight fold degeneracies in neutrino CP violation, mixing, and mass hierarchy, Phys. Rev. D **65,** 073023 (2002).

[5] K. Hagiwara and N. Okamura, Solving the degeneracy of the lepton-flavor mixing angle theta(ATM) by the T2KK two detector neutrino oscillation experiment, J. High Energy Phys. 01 (2008) 022.

[6] D. Meloni, Solving the octant degeneracy with the Silver channel, Phys. Lett. B **664,** 279 (2008).

[7] S. K. Agarwalla, S. Prakash, and S. U. Sankar, Resolving the octant of theta23 with T2K and NOvA, J. High Energy Phys. 07 (2013) 131.

[8] A. Chatterjee, P. Ghoshal, S. Goswami, and S. K. Raut, Octant sensitivity for large $\theta(13)$ in atmospheric and long baseline neutrino experiments, J. High Energy Phys. 06 (2013) 010.

[9] H. Minakata and S. J. Parke, Correlated, precision measurements of θ_{23} and δ using only the electron neutrino appearance experiments, Phys. Rev. D **87,** 113005 (2013).

[10] S. K. Agarwalla, S. Prakash, and S. Uma Sankar, Exploring the three flavor effects with future superbeams using liquid argon detectors, J. High Energy Phys. 03 (2014) 087.

[11] S. Choubey and A. Ghosh, Determining the octant of θ_{23} with PINGU, T2K, NOvA and reactor data, J. High Energy Phys. 11 (2013) 166.

[12] K. Bora, D. Dutta, and P. Ghoshal, Determining the octant of θ_{23} at LBNE in conjunction with reactor experiments, Mod. Phys. Lett. A **30,** 1550066 (2015).

[13] C. R. Das, J. Maalampi, J. Pulido, and S. Vihonen, Determination of the θ_{23} octant in LBNO, J. High Energy Phys. 02 (2015) 048.

[14] M. Ghosh, P. Ghoshal, S. Goswami, N. Nath, and S. K. Raut, New look at the degeneracies in the neutrino oscillation parameters, and their resolution by T2K, NOvA and ICAL, Phys. Rev. D **93,** 013013 (2016).

[15] N. Nath, M. Ghosh, and S. Goswami, The physics of antineutrinos in DUNE and determination of octant and δ_{CP}, Nucl. Phys. **B913,** 381 (2016).

[16] S. K. Agarwalla, S. S. Chatterjee, and A. Palazzo, Octant of θ_{23} in Danger with a Light Sterile Neutrino, Phys. Rev. Lett. **118,** 031804 (2017).

[17] N. Klop and A. Palazzo, Imprints of CP violation induced by sterile neutrinos in T2K data, Phys. Rev. D **91,** 073017 (2015).

[18] S. K. Agarwalla, S. S. Chatterjee, A. Dasgupta, and A. Palazzo, Discovery potential of T2K and NOvA in the presence of a light sterile neutrino, J. High Energy Phys. 02 (2016) 111.

[19] S. Choubey and D. Pramanik, Constraints on sterile neutrino oscillations using DUNE near detector, Phys. Lett. B **764,** 135 (2017).

[20] M. Ghosh, S. Gupta, Z. M. Matthews, P. Sharma, and A. G. Williams, Study of parameter degeneracy and hierarchy sensitivity of NOvA in presence of sterile neutrino, Phys. Rev. D **96,** 075018 (2017).

[21] S. Choubey, D. Dutta, and D. Pramanik, Imprints of a light sterile neutrino at DUNE, T2HK and T2HKK, Phys. Rev. D **96,** 056026 (2017).

[22] S. Choubey, D. Dutta, and D. Pramanik, Measuring the sterile neutrino CP phase at DUNE and T2HK, Eur. Phys. J. C **78,** 339 (2018).

[23] S. K. Agarwalla, S. S. Chatterjee, and A. Palazzo, Signatures of a light sterile neutrino in T2HK, J. High Energy Phys. 04 (2018) 091.

[24] S. Choubey, D. Dutta, and D. Pramanik, Exploring a new degeneracy in the sterile neutrino sector at long-baseline experiments, Eur. Phys. J. C **79,** 968 (2019).

[25] K. Abe *et al.* (Hyper-Kamiokande Collaboration), Physics potentials with the second Hyper-Kamiokande detector in Korea, Prog. Theor. Exp. Phys. **2018,** 063C01 (2018).

[26] K. Hagiwara, Physics prospects of future neutrino oscillation experiments in Asia, Nucl. Phys. B, Proc. Suppl. **137,** 84 (2004).

[27] M. Ishitsuka, T. Kajita, H. Minakata, and H. Nunokawa, Resolving neutrino mass hierarchy and CP degeneracy by two identical detectors with different baselines, Phys. Rev. D **72,** 033003 (2005).

[28] K. Hagiwara, N. Okamura, and K. i. Senda, Solving the neutrino parameter degeneracy by measuring the T2K off-axis beam in Korea, Phys. Lett. B **637,** 266 (2006); Erratum, Phys. Lett. B **641,** 491 (2006).

[29] K. Hagiwara, N. Okamura, and K. i. Senda, Physics potential of T2KK: An extension of the T2K neutrino oscillation experiment with a far detector in Korea, Phys. Rev. D **76,** 093002 (2007).

[30] T. Kajita, H. Minakata, S. Nakayama, and H. Nunokawa, Resolving eight-fold neutrino parameter degeneracy by two identical detectors with different baselines, Phys. Rev. D **75,** 013006 (2007).

[31] P. Huber, M. Mezzetto, and T. Schwetz, On the impact of systematical uncertainties for the CP violation measurement in superbeam experiments, J. High Energy Phys. 03 (2008) 021.

[32] K. Hagiwara and N. Okamura, Re-evaluation of the T2KK physics potential with simulations including backgrounds, J. High Energy Phys. 07 (2009) 031.

[33] F. Dufour, T. Kajita, E. Kearns, and K. Okumura, Further study of neutrino oscillation with two detectors in Kamioka and Korea, Phys. Rev. D **81,** 093001 (2010).

[34] K. Abe *et al.* (Hyper-Kamiokande Collaboration), Hyper-Kamiokande design report, arXiv:1805.04163.

[35] A. Badertscher, T. Hasegawa, T. Kobayashi, A. Marchionni, A. Meregaglia, T. Maruyama, K. Nishikawa, and A. Rubbia, A possible future long baseline neutrino and nucleon decay experiment with a 100 kton liquid argon TPC at okinoshima using the J-PARC neutrino facility, arXiv:0804.2111.

[36] K. Hagiwara, T. Kiwanami, N. Okamura, and K. i. Senda, Physics potential of neutrino oscillation experiment with a far detector in Oki Island along the T2K baseline, J. High Energy Phys. 06 (2013) 036.

[37] K. Hagiwara, P. Ko, N. Okamura, and Y. Takaesu, Revisiting T2KK and T2KO physics potential and ν_μ - $\bar{\nu}_\mu$ beam ratio, Eur. Phys. J. C **77**, 138 (2017).

[38] Y. Abe, Y. Asano, N. Haba, and T. Yamada, Heavy neutrino mixing in the T2HK, the T2HKK and an extension of the T2HK with a detector at Oki Islands, Eur. Phys. J. C **77**, 851 (2017).

[39] Z. Maki, M. Nakagawa, and S. Sakata, Remarks on the unified model of elementary particles, Prog. Theor. Phys. **28**, 870 (1962).

[40] B. Pontecorvo, Zh. Eksp. Teor. Fiz. **34**, 247 (1957) [Inverse beta processes and nonconservation of lepton charge, Sov. Phys. JETP **7**, 172 (1958)].

[41] M. Tanabashi *et al.* (Particle Data Group), Review of particle physics, Phys. Rev. D **98**, 030001 (2018).

[42] P. Adamson *et al.* (Daya Bay and MINOS Collaborations), Limits on Active to Sterile Neutrino Oscillations from Disappearance Searches in the MINOS, Daya Bay, and Bugey-3 Experiments, Phys. Rev. Lett. **117**, 151801 (2016); **117**, 209901(A) (2016).

[43] Y. Declais *et al.*, Search for neutrino oscillations at 15-meters, 40-meters, and 95-meters from a nuclear power reactor at Bugey, Nucl. Phys. **B434**, 503 (1995).

[44] P. Adamson *et al.* (MINOS Collaboration), Search for Sterile Neutrinos in MINOS and MINOS+ Using a Two-Detector Fit, Phys. Rev. Lett. **122**, 091803 (2019).

[45] M. G. Aartsen *et al.* (IceCube Collaboration), Searches for Sterile Neutrinos with the IceCube Detector, Phys. Rev. Lett. **117**, 071801 (2016).

[46] I. Esteban, M. C. Gonzalez-Garcia, A. Hernandez-Cabezudo, M. Maltoni, and T. Schwetz, Global analysis of three-flavour neutrino oscillations: Synergies and tensions in the determination of θ_{23}, δ_{CP}, and the mass ordering, J. High Energy Phys. 01 (2019) 106.

[47] I. Esteban, M. C. Gonzalez-Garcia, A. Hernandez-Cabezudo, M. Maltoni, and T. Schwetz, NuFIT 4.1 (2019), www.nu-fit.org.

[48] K. Abe *et al.* (Super-Kamiokande Collaboration), Limits on sterile neutrino mixing using atmospheric neutrinos in Super-Kamiokande, Phys. Rev. D **91**, 052019 (2015).

[49] J. Arafune, M. Koike, and J. Sato, CP violation and matter effect in long baseline neutrino oscillation experiments, Phys. Rev. D **56**, 3093 (1997); Erratum, Phys. Rev. D **60**, 119905 (1999).

[50] K. Hagiwara, N. Okamura, and K. i. Senda, The earth matter effects in neutrino oscillation experiments from Tokai to Kamioka and Korea, J. High Energy Phys. 09 (2011) 082.

[51] http://www.t2k.org/docs/talk/254/lmagalet.

[52] R. A. Smith and E. J. Moniz, Neutrino reactions on nuclear targets, Nucl. Phys. **B43**, 605 (1972); Erratum, Nucl. Phys. **B101**, 547 (1975).

[53] K. Abe *et al.* (Hyper-Kamiokande Proto- Collaboration), Physics potential of a long-baseline neutrino oscillation experiment using a J-PARC neutrino beam and Hyper-Kamiokande, Prog. Theor. Exp. Phys. **2015**, 53C02 (2015).